

The work described in this document was performed by Transportation Technology Center, Inc., a wholly owned subsidiary of the Association of American Railroads.

Analysis of Tie Plate Cracking Under Heavy Axle Loads

Potchara Tangtragulwong and Gary Fry, Texas A&M University
Richard Reiff and David D. Davis, TTCI

Summary

The Transportation Technology Center, Inc. and the AAR Affiliated Laboratory at Texas A&M University (TAMU) conducted an analysis of the effects of tie stiffness on tie plate cracking to determine the potential effects of tie material properties on the performance of tie-fastener systems.

This analysis was prompted by the observation of tie plate cracking on plastic composite ties at the Facility for Accelerated Service Testing (FAST), Pueblo, Colorado. Long-term testing showed that a significant number (i.e., ~10 percent) of the high rail tie plates in a test curve of plastic ties were cracking. Under the same operating conditions, solid sawn hardwood ties had few (i.e., <1 percent) cracked tie plates.

TAMU researchers built a finite element model of the wheel-rail-tie plate-tie structure to evaluate the effects of tie materials, loading and support conditions on the tie plate service environment. Heavy axle load conditions were modeled, including 136RE rail and AREMA 14 inch tie plates. A parametric study of tie bending stiffness was conducted using the model. The results were compared to field observations and measurements made on the High Tonnage Loop at FAST, and the following observations and conclusions were made:

- The model developed can be used as a design tool. The trends predicted from varying inputs, such as tie stiffness, match the field results obtained. However, further work is needed to properly calibrate the model, so that it can be used to accurately predict component lives. Tie plate bending stress will double for a composite tie with bending modulus that is 10 percent of wood ties.
- The effect of tie material on tie plate bending stresses is quite significant. Not only are bending stresses increased significantly with a less stiff tie, but the location of maximum stress changes.
 - Ties with lower bending stiffness (as compare to solid sawn hardwood ties) are more likely to have plate breakage at the spike holes.
 - Whereas, the wood ties will have maximum bending stresses near the plate end in curves. Wood ties are equally likely to have either plate spike hole or plate end fatigue in tangents.
- The properties of the ballast and subgrade foundation are relatively unimportant to tie plate bending strains. Reducing the ballast/subgrade support stiffness by 50 percent did not significantly affect the tie plate bending strains.

Future work will refine the inputs to the model, so that it can be accurately calibrated to measured performance data. Additional plate and fastener types can also be added.



INTRODUCTION

Plastic/composite ties are an option for replacement of wood ties because they have a higher resistance to decay and corrosion, they are compatible with the available fastening methods, and they are able to be intermixed with wood ties. However, recently, test engineers at FAST have found premature fatigue failures of tie plates installed on plastic/composite ties, while virtually no failures have been found in tie plates installed on wood ties.¹ The plate failures on plastic ties were located on the field side at the shoulder regions of ties on the high (outside) rail in curves.

From metallurgical inspection, crack initiation sites were located at the bottom corners of line spike holes, and then cracks propagated along the running direction until the tie plate fractured. This suggests that bending stresses in tie plates should play an important role in these high-cycle fatigue failures. Given an amount of wheel load, in-track tests on a 6-degree curve at FAST show that the larger tie plate bending stresses occur in the plastic/composite tie case.¹ This leads to a preliminary conclusion that tie plates installed on a less-stiff tie (plastic/composite) will experience more bending stresses, especially at bottom corners of the line spike holes on the field side and will be more susceptible to high-cycle fatigue failures.

Further, fretting toward the field side of the tie plate is evident in the failed components, suggesting possible importance of the lateral load acting on high rails. Transportation Technology Center, Inc. (TTCI) engineers developed a finite element model of tie plate bending to investigate the influence of elastic modulus of the ties and the amount of vertical and lateral loads on the bending stresses of the tie plates. A typical 36,000-pound (160kN) vertical load and 10,000-pound (45kN) lateral load were used in this study. Variation of these load levels also were used in the parametric studies.

Effect of Tie Material on Tie Plate Stresses

For the case of typical tie support and mainline traffic loading of 5,710 lbs/in (54kN/mm) vertical spring,² 36,000-pound (160kN) vertical load, and 10,000-pound (45kN) lateral load, deflections of tie plates installed on the wood and plastic ties are as Figure 1 shows.

Figure 2 shows the transverse stress contours (S_{zz}), under curving loads of the bottom surface of the tie plates for both wood and plastic tie cases.

Both the deflection and stress plots show the same effect. As tie bending stiffness is reduced, the field side spike hole areas of the tie plate are more highly stressed.

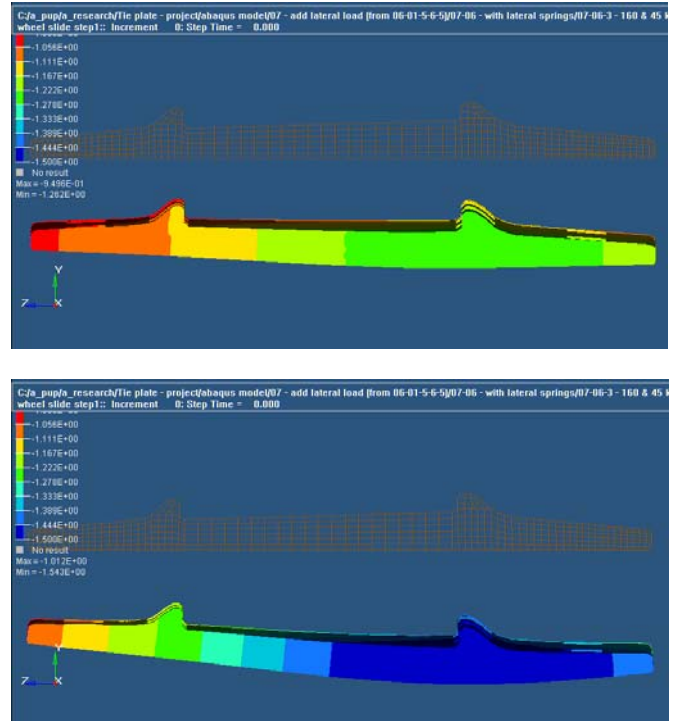


Figure 1: Deflections of the Tie Plates in Y of, (a) Wood E=1,740,000 psi (12GPa); (b) Composite E=174,000 psi (1.2GPa) (50X magnification)

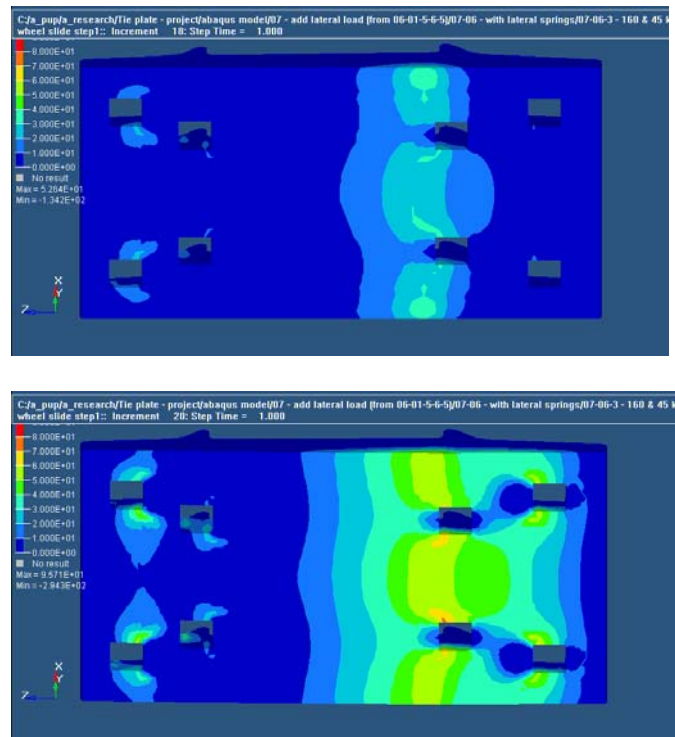


Figure 2: The Maximum Transverse Stresses of, (a) Wood E=1,740,000 psi (12GPa); (b) Composite E=174,000 psi (1.2GPa) (only the tensile stresses are shown)

Effects of Foundation Stiffness on Tie Plate Stresses

TAMU evaluated the effect of foundation stiffness over a wide range of likely tie support conditions. The effect on tie plate stresses was minimal, with virtually no effect on a representative plastic tie and a small effect on a stiffer wood tie. Figure 3 shows maximum transverse stress versus support stiffness for the wood and plastic ties. Also note that a stiffer tie (wood in this analysis) has much lower maximum plate stresses. Not evident in the plots was the shift in location of maximum stress between tie types. For the less stiff tie, the location of maximum stress is in the field side spike holes. For the stiffer tie, the location is near the field side edge of the tie plate.

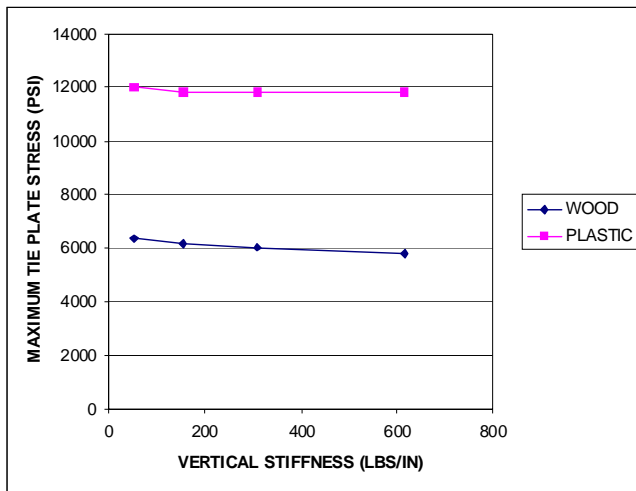


Figure 3. Maximum Transverse Stress vs. Tie Support Stiffness

Wheel-Rail-Tie Plate-Tie Model

TAMU developed a finite element model of the wheel-rail-tie plate-tie on an elastic foundation for this study. The contact models, being nonlinear, required considerable computation capacity, therefore Texas A&M University provided the supercomputers used to run the model.

The model consisted of five main parts in full-scale: (1) axle, (2) wheel, (3) rail with extended beams, (4) tie plate, and (5) tie. Figure 4 shows the assembled model. The wheel and rail models were meshed with variable element densities as the very fine elements were located at the contact region of wheel and rail models, whereas the element size was increased proportionally while moving away from the contact region. The mismatches of different element size in wheel and rail models were controlled by the TIE command in ABAQUS® version 6.5 to guarantee compatible displacement of the tied surfaces of different element sizes.³

The tie plate profile was measured directly from the test specimen used by TTCL. The front and top view of the tie plate model is as Figure 5 shows. The tie model’s cross section of 5 inch x 10 inch (125x250mm²) was extruded to 51 inches (1,300 mm), half of the total length of a typical tie, to take an

advantage of symmetry along the running direction. Higher element density was used in the region making contact with the tie plate’s base.

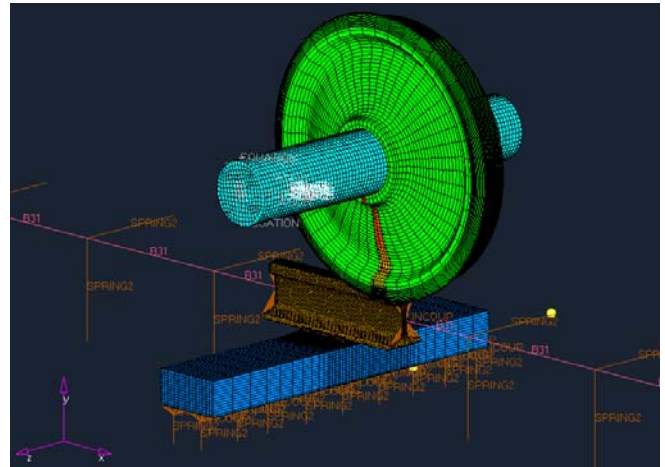


Figure 4: Finite Model showing the Axle, Wheel, Rail, Tie Plate, and Vertical and Lateral Springs

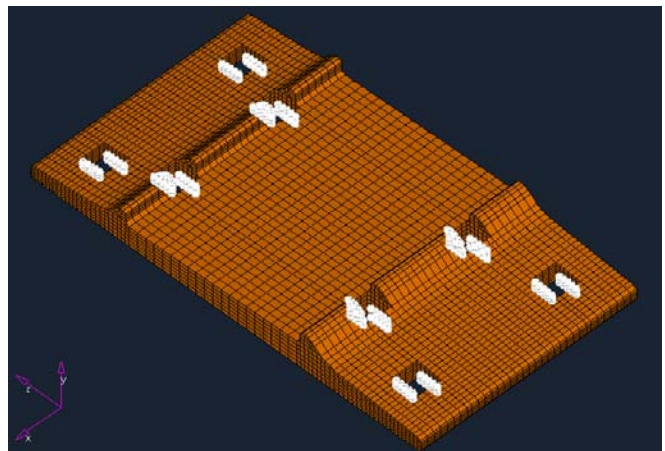
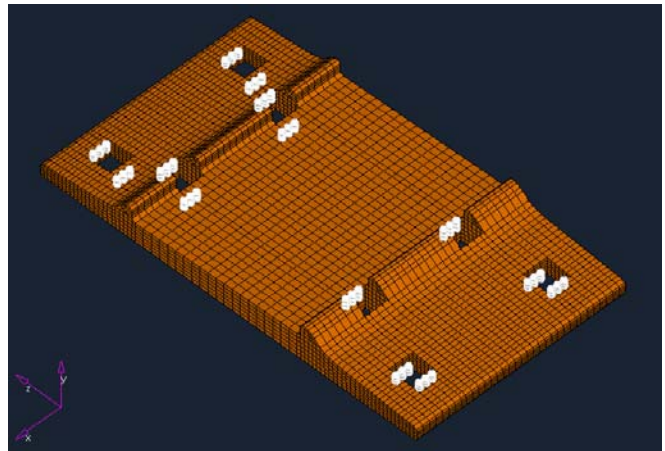


Figure 5: Boundary Conditions Proposed for use in All Simulations

Spring elements with stiffness of 5,710 lbs/in (54kN/mm) representing the ballast materials and substructure were vertically connected to a tie and beam's nodes as Figure 1 shows. Similarly, to represent the lateral resisting force that the tie plate acting on the rail's base, springs with varied stiffness (depending on the elastic modulus of the tie) were connected to the beam's node in lateral direction.

According to Darris, as the train runs through the 6-degree curve rail, the 10,000-pound (45kN) lateral force, toward the high rail of field side, will transfer from the wheel-rail contact to the rail's base-tie plate's ridge contact.⁴ This lateral force will be resisted eventually by the boundary conditions applied on the spike holes, which will allow the rail's center of gravity to slightly move in lateral direction.

From the simulations with only the 23.6 inch (600 mm) solid-element rail section, results of the lateral displacement for each case of elastic modulus will be used to calculate "virtual" lateral stiffness, according to the Hooke's law (strength of materials).

Because the beam elements extended from the solid-element rail ends alone could not simulate the reaction force from the tie plate's ridge acting on the rail's base, the springs with calculated lateral stiffness will be imposed on all beam's nodes instead.

The simulation steps defined below are with the axle-wheel unit located at the mid-length of rail at the beginning of the simulations.

- Step 1: Apply the vertical displacement of 0.004 inch (0.1 mm) to the axle node to initiate a firm contact between wheel and rail surfaces.
- Step 2: Activate the gravity to make the mass element active.
- Step 3: Deactivate the vertical displacement applied in Step 1. Keep only the effect from mass element.
- Step 4: Allow the displacement of the axle nodes on the symmetry plane, and apply the 10,000-pound (45kN) lateral force onto these axle nodes instead. The orientation of this symmetry plane must always parallel to the running direction.
- Step 5: Measure the displacement of the rail's center of gravity.

As the tie plate displaces from the wheel sliding over the rail, this type of fastener will resist the lateral displacement of the tie plate with compressive force only, assuming that the spikes are more rigid/ or as rigid as the tie plate. Therefore, the boundary conditions applied to the spike holes must create only the compressive stresses.

The simulations proceeded following the steps below with the boundary conditions on spike holes that (1) prevented the side of the spike holes oriented along the x-direction from displacement in z-direction, and (2) prevented the side of the spike holes oriented along the z-direction from displacement in x-direction (see Figure 5). The center node of the axle was located at + 9.61 inches (244 mm) from the mid-length of the rail in longitudinal direction as the simulation began.

Step 1-4: Same as those above

Step 5: With the application of the 10,000-pound (45kN) lateral force and 36,000-pound (160kN) vertical force, slide the axle-wheel unit along the running direction for -19.2 inches (488 mm) until the axle-wheel stops at the opposite end of the solid-element rail section.

FUTURE WORK

This design and analysis tool will be calibrated to provide more accurate service life predictions. Additional plate and fastener configurations will be added.

The track component models developed in this study can be used to design improved performance tie/fastener and track systems. This type of tool can be used to assess the likely failure modes of components and to develop methodologies to mitigate these failure modes. Economic analysis of alternatives can also be conducted to determine lowest life-cycle cost designs.

REFERENCES

1. Gonzales, Kari et al. February 2008. "Evaluation of Tie Plate Cracking on Composite Ties." *Technology Digest*, TD-08-009, Association of American Railroads, Transportation Technology Center, Inc., Pueblo, Colorado.
2. Esveld, C., Professor. 2001. *Modern Railway Track*. 2nd Ed. Delft University of Technology. MRT-Productions, The Netherlands.
3. Hibbit, Karlsson, and Sorensen Inc. 2006. ABAQUS® User's Manual 6.5, Providence, Rhode Island.
4. Darris, W.L. 1998. "Statistical Characterization of Vehicle and Track Interaction Using Rail Vehicle Response and Track Geometry Measurements." Master's Thesis, Mechanical Engineering Department, Virginia Polytechnic Institute and State University, Blacksburg, Virginia.

Visit our website at <http://www.ttc.aar.com>